International Journal of Mathematics and Statistics

ISSN (Online): 2208-2212
Volume 10 Issue 02 June 2024

DOI: https://doi.org/10.69980/y9gqaa47

STATISTICAL CHARACTERIZATION AND MULTIVARIATE MODELING OF ELECTROCHEMICAL POLARIZATION RESPONSE VARIABILITY

Dr. Nathaniel R. Collins[1*], Prof. Isabelle M. Laurent[2], Dr. Hiroshi K. Yamamoto[3], Dr. Daniel A. Fischer[4]

[1]Department of Electrochemical Engineering and Statistical Analysis, Westbridge University of Technology, Manchester, United Kingdom*
[2]Institute of Materials Science and Electrochemical Research, École Nationale des Sciences Appliquées, Lyon, France
[3]Department of Chemical Engineering and Applied Statistics, Kyoto Institute of Technology, Kyoto, Japan
[4]School of Data Science and Corrosion Engineering, Rhine Technical University, Düsseldorf, Germany

Abstract:

Electrochemical polarization curves encode quantitative data about response size, response dispersion, integrated response behavior and gradient characteristics, but these attributes are most often studied individually instead of in an integrated statistical framework. This study aimed to characterize polarization-response variability across experimental conditions and identify the dominant multivariate structure of curve-derived numerical features. A total of 955 polarization curves across five NaCl concentration and scan-rate conditions were analyzed. Descriptive statistics, Kruskal-Wallis test with epsilon-squared effect sizes, log-transformation regression modeling, principal component analysis, and sensitivity analysis (with ≥95% curve completeness) were analyzed. All principal characteristics differed significantly across experimental conditions ($p<0.001$), with epsilon-squared values ranging from 0.257 to 0.489. Mean absolute slope showed the strongest between-condition separation and the highest regression fit ($R2=0.509$). PC1 explained 90.583% of the total variance, while PC1 and PC2 jointly accounted for 97.274%. Sensitivity analysis produced comparable statistical and multivariate patterns. The results show that numerical feature extraction combined with inferential, regression, and multivariate methods is a concise and powerful approach to characterise the variability in electrochemical polarization-response.

Keywords: *electrochemical polarization, statistical modeling, numerical characterization, principal component analysis, response variability*

1. Introduction

The polarization curves of an electrode couple can be measured in an electrochemical cell and are quantitative results that show the relationship between the applied potential and the measured current density and can be used to study the changes in the electrochemical response taking place at the electrode interfaces over a controlled potential range. The shape, magnitude, transition regions and gradients of these contain information that can sometimes not be expressed adequately in one response value. Polarization-based measurements are therefore widely used for electrochemical characterization which allows a systematic study of reaction behaviour and material response under desired experimental conditions (Choudhary et al., 2017). The interpretation of these curves is based on relationships between potential, current, charge transfer process, mass transport, and electrode kinetics and therefore numerical treatment of the measured curve is crucial when the curves show significant variation (Eliaz & Gileadi, 2019).

The magnitudes of an electrochemical response and its shape can change with experimental conditions. The composition of the electrolyte is especially important, since the ionic concentration may affect transport phenomena and the environments of the interfaces and reaction rates. Previous studies of concentrated electrolytes have shown that the variation in the response can be different for different electrolyte concentrations, highlighting the significance of studying the response variation at different electrolyte concentrations (Hu et al., 2021). The third measurement condition for which polarization results are important is called the scan rate, that is, the rate at which the potential is scanned. Polarization curves have been tested in the laboratory by Hung et al. (2017), and it has been demonstrated that measurable scan-rate dependence exists, thereby allowing for a deliberate inclusion of the scan rate in the analysis of the characteristics of the polarization curve. A statistical description over such conditions may thus be more comprehensive than one based on the individual curves.

Finally, polarization curves are also an analytical problem, since they involve numerous sequential data points and can show different characteristics for successive measurements. An application of extraction of structured information from the full response profile of polarization measurements has been explored in the context of curve decomposition in electrochemical measurements (Strebl et al., 2023). Another difficulty is that there may be two types of variation: a systematic pattern and a potentially significant local variation, which is created by stochastic variation. When variability in the data is important to the problem, such data should be interpreted in a quantitative way that is suitable, as highlighted by Jamali et al. (2024). The reasons for this give support to the idea of representing each curve as a numerical quantity that can be extracted from and compared with other curves on a statistical basis.

The growing popularity of the use of statistical techniques in connection with electrochemical analysis provides a means of dealing with this complexity. Robinson and Sigman (2020) showed how electrochemical measurements and statistical tools may be coupled to improve the quantitative interpretation and mechanistic investigation. It has been observed that the development of electrochemical impedance analysis has shifted towards the use of computational approaches that can obtain distributed information instead of relying on the classic parameters summarizing the response (Maradesa et al., 2024). The analytical–computational approach has also been used to enhance quantitative analysis of electrochemical measurements by fitting models, optimizing parameters and performing statistical validation (Nuñez Perez, 2025). These developments show a general shift to electrochemical analysis based on data and numbers rather than one that is interpretative, with data being represented numerically and evaluated statistically alongside existing interpretation.

Multivariate analysis is particularly pertinent when a number of curve-derived characteristics are related to aspects of the same response. The combination of electrochemical measurements with multivariate statistical analysis has been employed to identify and classify complex patterns in samples and to simplify the multidimensional information into meaningful patterns (Geană et al., 2020). PCA is a mathematical tool that can be used to model correlated variables by a smaller set of orthogonal variables that preserve a significant amount of variation in the original variables. This is a method that has been well developed in multivariate statistics to select dominant covariance structure and derive lower-dimensional representations of high-dimensional numerical observations (Mardia et al., 2024). The increasing evolution of multivariate data analysis has also highlighted the importance of considering the association between sets of variables as a whole rather than interpreting the measures of association between variables separately (Black & Babin, 2019).

However, there is a methodological gap in the integrated statistical characterisation of the variability of polarization curves. While attention given to selected physical parameters or individual response profiles is common electrochemical analyses, attention given to a single curve-level framework of numerical feature extraction, distribution-sensitive statistical comparisons, regression modelling and multivariate dimensionality reduction is less common. The behavior of the response magnitude, response dispersion, the area under the curve and the gradient characteristics of the response as a function of the concentration and scan-rate conditions should also be systematically evaluated. There is also a need to check for the stability of statistical structures when only highly complete curves are analysed, because this is not necessarily the case when differences in measurement completeness exist. Solving these problems can make polarization measurements more reliable when used in a quantitative manner and place the electrochemical system in a class of applications where statistical and numerical methods are used.

The aim of the present study is thus to statistically describe and model the variability of electrochemical polarization response under experimental conditions. The first goal is to measure the central tendency, dispersion, integrated response and gradient characteristics with numerical features at the level of the curve. The second goal is to assess differences and statistical correlations between principal polarization characteristics in different concentrations and scan rates for electrolytes. The third aim is to discover dominant multivariate patterns by means of principal component analysis and to evaluate the stability of the structure derived from the statistical analysis to the incompleteness of the measurements.

2. Methodology

2.1 Research Design

A quantitative computational design method was chosen to describe the polarization curves of the electrochemical system using statistical and multivariate methods. Each polarization curve was analysed independently for numerical characterization. The analytical framework included data preprocessing, curve-level feature extraction, descriptive data, non-parametric testing, regression modelling, principal component analysis (PCA) and sensitivity assessment. This allowed for a systematic assessment of the polarization characteristics over the experimental conditions without making the analysis at the level of individual raw measurement points.

2.2 Data Source

These data were measured from the experimental work reported by Coelho (2023). Records were made of potentio-dynamic polarisation data taken from 316L stainless steel at different concentrations of NaCl and scan rates. For each polarization curve, two sets of potential and current-density values were obtained, each with sufficient points to be numerically characterized and modelled using a statistical approach.

2.3 Data Preparation and Quality Assessment

The potential and current density records were matched based on their experimental conditions and sorted at the curve level. Data integrity was evaluated by checking dimensional consistency, missing readings, non-finite readings, and the number of valid potential-current pairs. Observations of current density that were missing were not imputed and were considered missing. The proportions of valid observations to the estimated number of observations were computed for curve-level completeness. Furthermore, a criterion of completeness of ≥95% was set as an additional completeness criterion for the robustness assessment.

2.4 Numerical Characterization of Polarization Curves

Valid potential–current pairs were used to transform each polarization curve into a set of numerical descriptors. The characteristics that were extracted were minimum current, maximum current, mean current, median current, mean absolute current, current standard deviation and current range. The total area under the curve (AUC) was quantified, with a trapezoidal numerical integration used. The mean absolute slope (MAS) was used to represent the curve-gradient behavior as defined by the mean value of the absolute gradient of current density with respect to potential change between successive points. These descriptors were used to give numerical descriptions of curve magnitude, dispersion, integrated response and gradient variation, which were standardized.

2.5 Descriptive and Inferential Statistical Analysis

The data were analysed using descriptive statistics for each experimental condition. Due to the curvature of the characteristics and the large differences in the magnitude of the responses, median and quartile ranges were used as the main summary measures. The mean absolute current, the standard deviation of the current, the range of the current, the absolute area under the curve (AUC), and the mean absolute slope were tested for differences between the conditions using the Kruskal–Wallis test. Statistical significance was assessed at $p<0.05$. Epsilon-squared ($\varepsilon 2$) was calculated to quantify the magnitude of differences identified by the non-parametric comparisons.

2.6 Regression Modeling

The regression models were created individually for mean absolute current, standard deviation of current, range of current, absolute AUC, and mean absolute slope. Data were log-transformed prior to the model because they were positively skewed and were prone to numerical instability. The experimental conditions of NaCl concentration and scan rate were included as explanatory factors. The model performance was evaluated using the coefficient of determination (R2), adjusted R2, F statistic, and associated significance level. Model coefficients were considered conditional associations because the experimental conditions did not constitute a complete factorial combination of concentration and scan rate.

2.7 Principal Component Analysis

The common variation between the main characteristics derived from the principal curve was explored using PCA. The data were transformed to a logarithmic scale and standardized before analyses to correct for differences in scales and dispersion: mean absolute current, current standard deviation, current range, absolute AUC, and mean absolute slope. The feature matrix was standardized and then principal components were extracted. The values of eigenvalues and explained variance were obtained for each component, and the component scores were used to explore the distribution of curves in reduced dimensional space. The feature loadings were calculated to see the relative contribution of each numerical feature to the principal components.

2.8 Sensitivity Analysis

The robustness of the findings was assessed by repeating the main analyses after restricting the analytical sample to curves with ≥95% completeness. The Kruskal–Wallis tests and corresponding epsilon-squared estimates were re-computed with the restricted sample. The same logarithmic transformation and standardisation were also repeated for PCA. Several changes in inferential statistics, effect sizes, explained variance, and component loadings were explored to determine the robustness of the analytic results for incomplete curve observations.

3. Results

3.1 Data Quality and Analytical Sample

A total of 955 polarization curves were obtained in the end under five experimental conditions. According to Table 1, the number of curves recorded varied from 47 curves (0.050 M NaCl at 50 mV/s) to 377 curves (0.010 M NaCl at 100 mV/s). In the four conditions, the mean value of completeness was above 99% except for 0.050 M at 100 mVs-1 (94.59%). In total, 935 curves (97.91%) reached a completeness of ≥95%. The number of valid points per curve was also found to be different depending on the scan rate, with values of around 2,217–2,218 at 50 mV/s and 1,103–1,108 at 100 mV/s.

Table 1. Dataset and data-quality characteristics

NaCl (M)	Scan rate (mV/s)	Curves	Median valid points	Mean completeness (%)	Minimum completeness (%)	Curves ≥95% complete	Curves ≥95% complete (%)
0.005	100	287	1108	100.00	99.64	287	100.00
0.010	50	119	2218	99.90	95.13	119	100.00
0.010	100	377	1108	100.00	100.00	377	100.00
0.050	50	47	2217	99.51	93.23	46	97.87
0.050	100	125	1103	94.59	29.72	106	84.80

3.2 Distribution of Polarization Characteristics

The numerical features extracted were found to be very different for various experimental conditions. Table 2 shows that median mean absolute current ranged from 794.95 at 0.010 M and 100 mV/s to 39,831.29 at 0.050 M and 50 mV/s. Median current range varied from 7,829.76 to 543,160.70, while median absolute AUC ranged from 676.26 to 33,909.70. Mean absolute slope showed the widest numerical separation, ranging from 46,093.14 at 0.010 M and 100 mV/s to 1,259,243.12 at 0.050 M and 50 mV/s. The distributions of absolute AUC for each of the conditions are shown in Figure 1A, where the highest median and broadest range are found at 0.050 M and 50 mV/s, respectively. The distributions of mean absolute slope were highest at 0.050 M and 50 mV/s, and were lowest at 0.010 M and 100 mV/s (Figure 1B).

Table 2. Descriptive statistics of principal polarization features

NaCl (M)	Scan rate (mV/s)	N	Mean absolute current, median	Mean absolute current, IQR	Current range, median	Current range, IQR	Absolute AUC, median	Absolute AUC, IQR	Mean absolute slope, median	Mean absolute slope, IQR
0.005	100	287	1,523.81	994.25	10,452.63	3,069.40	1,290.63	848.72	74,379.62	59,562.39
0.010	50	119	1,446.04	1,783.34	12,686.93	46,973.71	1,232.86	1,522.94	158,695.45	160,453.53
0.010	100	377	794.95	141.91	7,829.76	2,214.87	676.26	120.52	46,093.14	5,798.61
0.050	50	47	39,831.29	167,975.16	543,160.70	1,169,371.13	33,909.70	141,793.75	1,259,243.12	2,772,811.46
0.050	100	125	1,926.95	2,409.73	79,521.62	110,364.65	1,600.32	1,966.44	257,135.33	479,638.77

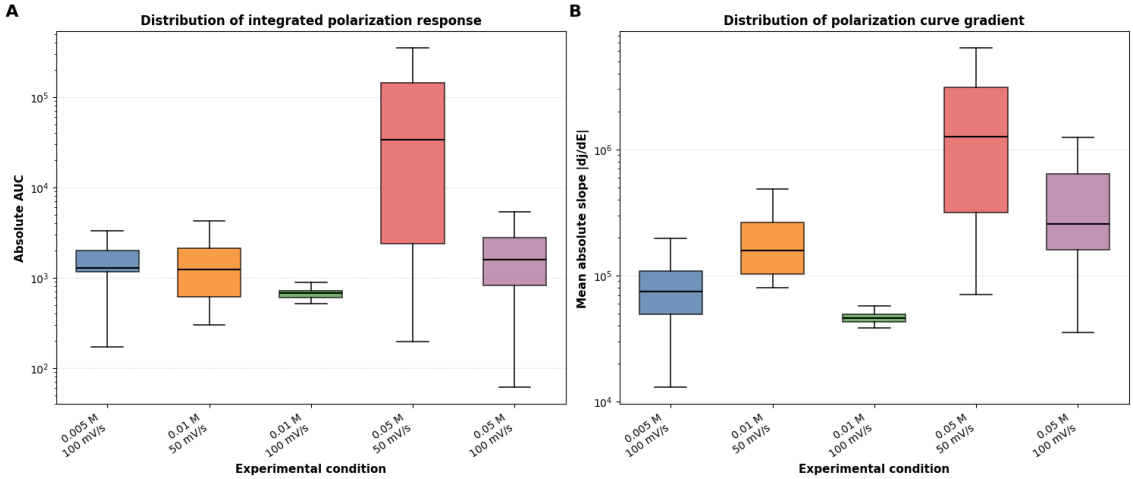

Figure 1. Distribution of numerical polarization characteristics across experimental conditions. (A) Integrated polarization response represented by absolute AUC. (B) Polarization curve gradient represented by mean absolute slope.

3.3 Differences Across Experimental Conditions

Every characteristic was determined by Kruskal–Wallis testing, and there were significant differences in the five experimental conditions. As seen in Table 3, all tests were significant at $p<0.001$. For the H statistics, the mean absolute current was 279.249, and the current standard deviation was 268.770; the current range was 247.720; the absolute AUC was 275.617, and the mean absolute slope was 468.239. The range of values of epsilon-squared was 0.257 to 0.489. The sensitivity analysis for completeness ≥95% kept 935 curves. All five comparisons were significant at $p < 0.001$, with epsilon-squared values between 0.291 and 0.503.

Table 3. Primary and sensitivity Kruskal–Wallis results

Feature	Primary N	Primary H	df	Primary p	Primary ε^2	Sensitivity N	Sensitivity H	Sensitivity p	Sensitivity ε^2
Mean absolute current	955	279.249	4	<0.001	0.290	935	300.387	<0.001	0.319
Current SD	955	268.770	4	<0.001	0.279	935	288.957	<0.001	0.306
Current range	955	247.720	4	<0.001	0.257	935	274.627	<0.001	0.291
Absolute AUC	955	275.617	4	<0.001	0.286	935	298.063	<0.001	0.316
Mean absolute slope	955	468.239	4	<0.001	0.489	935	471.930	<0.001	0.503

3.4 Regression Model Results

The log-transformed polarization characteristics regression models were all statistically significant. Table 4 shows R2values of 0.276 for mean absolute current, 0.271 for current standard deviation, 0.288 for current range, and 0.265 for absolute AUC. The highest R2was obtained for mean absolute slope at 0.509, with an adjusted R2of 0.507. F statistics ranged from 49.602 to 149.549, with $p<0.001$for all models.

Table 4. Regression model performance for polarization characteristics

Outcome	N	R^2	Adjusted R^2	F statistic	p-value
Mean absolute current	955	0.276	0.273	79.053	<0.001
Current SD	955	0.271	0.269	49.602	<0.001
Current range	955	0.288	0.286	51.361	<0.001

Absolute AUC	955	0.265	0.263	78.348	<0.001
Mean absolute slope	955	0.509	0.507	149.549	<0.001

3.5 Principal Component Analysis

Most of the variance in the standardized numerical features was explained by the first two principal components. From Table 5, it can be seen that the first principal component (PC1) accounted for 90.583% of the total variance with an eigenvalue of 4.534. The eigenvalue of PC2 was 0.335, and it accounted for another 6.691%, bringing the cumulative explained variance to 97.274%.

Table 5. Principal component analysis summary

Principal component	Eigenvalue	Explained variance (%)	Cumulative variance (%)
PC1	4.534	90.583	90.583
PC2	0.335	6.691	97.274

The scores of all 955 curves in the PC1–PC2 plane are plotted in Figure 2. Mean PC1 scores were −0.111 for 0.005 M/100 mV/s, 0.250 for 0.010 M/50 mV/s, −0.978 for 0.010 M/100 mV/s, 4.400 for 0.050 M/50 mV/s, and 1.311 for 0.050 M/100 mV/s. The corresponding mean PC2 scores were −0.363, 0.491, −0.101, 0.031, and 0.660, respectively.

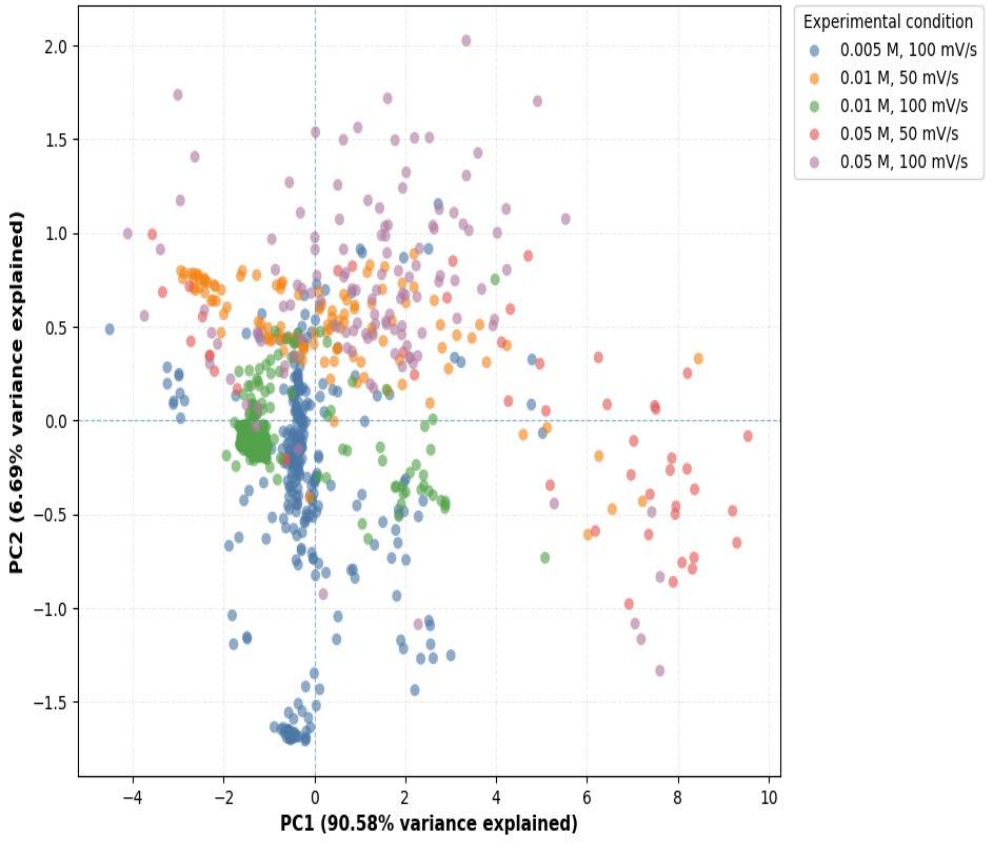

Figure 2. Principal component scores of polarization curves across experimental conditions.

3.6 Principal Component Loadings

The loading coefficients indicated the relative importance of the five numerical variables to PC1 and PC2. As seen in Figure 3, mean absolute current (0.455), current standard deviation (0.465), current range (0.453), absolute AUC (0.453) and mean absolute slope (0.407) had positive PC1 loadings. Mean absolute slope had the highest positive loading (0.827) for PC2, followed by current range (0.112). The loadings of PC2 were −0.374 for mean absolute current, −0.081 for current standard deviation and −0.398 for absolute AUC.

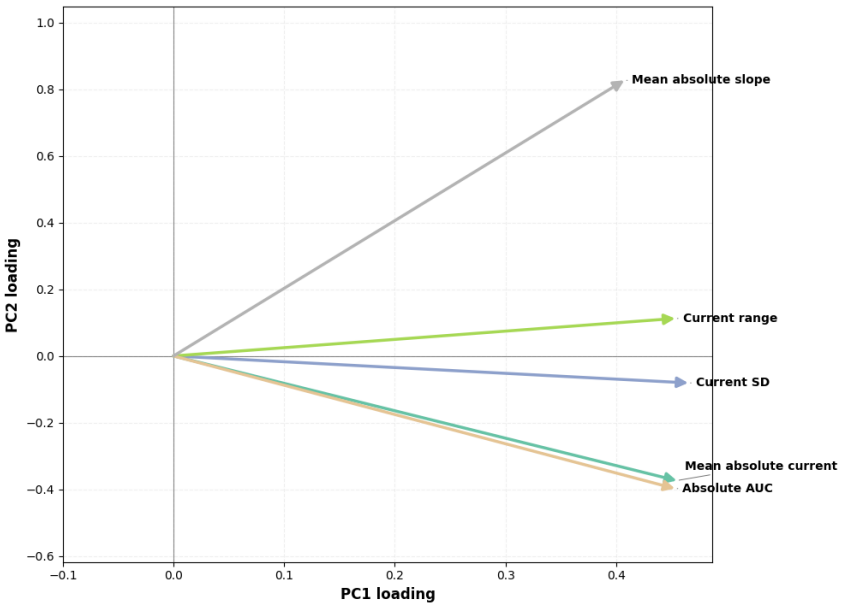

Figure 3. Principal component loading structure of polarization features.

4. Discussion

The polarization responses showed strong condition-dependent differences in both the magnitude and dispersion, as well as in the integrated response and gradient of the curve. The median mean absolute current, mean absolute slope, current range, and absolute AUC were all found to be highest at the 0.050 M NaCl condition, with the lowest being at 0.010 M NaCl, and all at 100 mV/s. The interquartile ranges of the data were also large, at 0.050 M and 50 mV/s, suggesting larger within-condition variability, especially for current range and mean absolute slope. The curves indicate that the changes in experimental conditions were manifested at the same time in several numerical characteristics of the polarization curve. The Kruskal–Wallis test showed significant differences among all five conditions (εpsilon-squared from 0.257 to 0.489). The largest effect size was from Mean absolute slope in terms of the effect on curve-gradient behavior. A sensitivity analysis yielded similar results when the curves were limited to those that are at least 95% complete, showing that the remaining curves did not significantly affect the statistical pattern. Regression modeling provided an additional assessment of variability across experimental conditions. The models accounted for about 26.5–28.8% of the variance in the mean absolute current, the standard deviation of current, the range of current, and the absolute AUC, respectively, with a model for the mean absolute slope having an R^2 of 0.509. The multivariate structure was extremely concentrated, with the first two PCs accounting for 97.274% of the total variance, with the first one accounting for 90.583%. The common variance of all five features was identified by the positive loadings on PC1, and the high loading on PC2 for mean absolute slope differentiated them from other features, as it varied according to the gradient.

The difference seen between the various electrolyte conditions is consistent with other evidence that the concentration of the electrolyte can have a significant effect on the polarization behavior. The sensitivity of polarization response to the electrolyte concentration was demonstrated by Chen et al. (2025), who optimized the electrolyte concentration to reduce the electrode polarization. Similar results were published by Zhu et al. (2024) and they revealed that the electrochemical performance of hydrogel electrolytes varied as a function of the concentration of both water and salt. The electrochemical systems are different, but both studies confirm that there is a significant amount of response variation due to concentration. It is noted that the curve-level statistical method is consistent with the previous one, which specifically included 316L stainless steel. Coelho et al. (2023) showed the usefulness of statistical and machine-learning analysis to estimate the pitting descriptors based on electrochemical measurements. The present results support that approach by demonstrating that numerical representations of magnitude, dispersion, integrated response and gradient can all describe the variability in polarization. Other electrochemical systems have also shown variability to be a useful analysis parameter. When there is inconsistency in the response to a stimulus, Wang et al. (2025) quantified and predicted the inconsistencies in lithium-ion battery packs from operating data, highlighting the importance of statistical characterization. A similar finding of spatiotemporal variation in polarization was also found by Suzer et al. (2021) in operando potential mapping, highlighting the need to consider electrochemical heterogeneity.

The regression results are consistent with the general trend of using multivariable statistical models for assessing the electrochemical response. In an effort to estimate the lithium-ion battery state of health, Lyu et al. (2022) implemented a Bayesian multivariate regression model with several health indicators. The types of such work help in bringing together related numerical indicators, instead of evaluating them individually. Evidence of structured, multidimensional variation in polarization behavior is also found to be in agreement with the PCA results. Sun et al. (2025) applied time-resolved electrochemical measurements to characterize the distribution of dynamic polarization behavior, finding that polarization responses may exhibit different patterns for different operating states and indicating that distinguishable polarization patterns are available. Del Zotto et al. (2024) also demonstrated that parameterized polarization losses can aid in the prediction of the current–voltage characteristics. These studies agree that reduced number representations are suitable for electrochemical responses.

The results show the usefulness of the combined use of numerical curve characterization, inferential and multivariate statistics. Polarization features derived from the curve allow complete polarization profiles to be translated into meaningful and quantitative polarization parameters, and non-parametric testing allows comparison of different trends of response, which are heterogeneous. The condition associated variation can be quantified by regression modeling, and the PCA representation can be used to provide a compact representation of correlated polarization characteristics. The high percentage of variance explained by the first two principal components indicates that there is a lot of variance at the curve level that can be captured in an economical manner without adding a new dimension for each of the curve's characteristics. In this work, a statistical applied approach to analyze collections of electrochemical response curves is proposed, maintaining most of the main statistical characteristics of the curves.

There are some restrictions to be noted. The experimental groups were not matched, and the concentration and scan rate were not a complete factorial design. A small proportion of curves contained incomplete current-density measurements; however, sensitivity analysis restricted to curves with ≥95% completeness produced comparable statistical patterns. The framework developed in this work could be used in future studies for balanced experimental designs, expanded concentration and scan rates, and in stand-alone electrochemical systems. The statistical structure identified may also be studied in conjunction with other curve descriptors and/or nonlinear multivariate methods to analyze whether they can account for other components of the polarization variability that are not captured by the statistical structure.

5. Conclusion

The electrochemical polarization responses showed a significant spread when the different NaCl concentration and scan-rate conditions were tested. The responses were characterized numerically at the curve level, where there were significant differences in the amplitude of the response, its dispersion, the integrated area of the response and its gradient behavior with the best curve-level differentiation being in terms of mean absolute slope. Non-parametric comparisons revealed that all main polarization characteristics were different between groups and the sensitivity analysis demonstrated that these trends did not change with the inclusion of only very complete curves. Regression modeling showed that the experimental factors explained meaningful variation in the numerical features extracted from the polarization curves, with the strongest explanatory performance observed for mean absolute slope. PCA can effectively reduce the multivariate feature space, with PC1 explaining 90.583% of total variance and the first two components explaining 97.274% of the total variance. The results demonstrate the usefulness of numerical feature extraction, inferential statistics, regression and multivariate analysis for characterizing the variability in the polarization responses in a compact and robust framework. The method is useful for quantitative electrochemical analysis and applies to a wider range of experimental conditions and other electrochemical systems.

References:

[1]. Black, W., & Babin, B. J. (2019). Multivariate data analysis: Its approach, evolution, and impact. In The great facilitator: Reflections on the contributions of Joseph F. Hair, Jr. to marketing and business research (pp. 121-130). Cham: Springer International Publishing.

[2]. Chen, W., Wang, K., He, X., Chen, X., Huang, T., Chen, J., ... & Hu, J. (2025). Mitigating electrode polarization through electrolyte concentration optimization. Nano Energy, 139, 110950.

[3]. Choudhary, Y. S., Jothi, L., & Nageswaran, G. (2017). Electrochemical characterization. In Spectroscopic Methods for Nanomaterials Characterization (pp. 19-54). Elsevier.

[4]. Coelho, L. B. (2023). Micro-scale potentiodynamic polarisation curves of 316L stainless steel [Data set]. Mendeley Data. https://doi.org/10.17632/78rz8vw46x.2

[5]. Coelho, L. B., Torres, D., Vangrunderbeek, V., Bernal, M., Paldino, G. M., Bontempi, G., & Ustarroz, J. (2023). Estimating pitting descriptors of 316 L stainless steel by machine learning and statistical analysis. NPJ Materials Degradation, 7(1), 82.

[6]. Del Zotto, L., Tamburrano, G., Dell'Era, A., Hatunoglu, A., & Ciro, E. (2024). Determination and validation of polarization losses parameters to predict current/voltage-characteristics for SOFC button cell. Energy Conversion and Management, 299, 117877.

[7]. Eliaz, N., & Gileadi, E. (2019). Physical electrochemistry: fundamentals, techniques, and applications. John Wiley & Sons.

[8]. Geană, E. I., Ciucure, C. T., & Apetrei, C. (2020). Electrochemical sensors coupled with multivariate statistical analysis as screening tools for wine authentication issues: A review. Chemosensors, 8(3), 59.

[9]. Hu, J., Guo, H., Li, Y., Wang, H., Wang, Z., Huang, W., ... & Pan, F. (2021). Understanding Li-ion thermodynamic and kinetic behaviors in concentrated electrolyte for the development of aqueous lithium-ion batteries. Nano Energy, 89, 106413.

[10]. Hung, Y., Bu, Y., Kubin, J., & Weinman, D. (2017, October). Effects of current scan rate on the polarization curve of vanadium redox flow batteries. In 2017 International Energy and Sustainability Conference (IESC) (pp. 1-4). IEEE.

[11]. Jamali, S. S., Wu, Y., Homborg, A. M., Lemay, S. G., & Gooding, J. J. (2024). Interpretation of stochastic electrochemical data. Current Opinion in Electrochemistry, 46, 101505.

[12]. Lyu, Z., Wang, G., & Tan, C. (2022). A novel Bayesian multivariate linear regression model for online state-of-health estimation of Lithium-ion battery using multiple health indicators. Microelectronics Reliability, 131, 114500.

[13]. Maradesa, A., Py, B., Huang, J., Lu, Y., Iurilli, P., Mrozinski, A., ... & Ciucci, F. (2024). Advancing electrochemical impedance analysis through innovations in the distribution of relaxation times method. Joule, 8(7), 1958-1981.

[14]. Mardia, K. V., Kent, J. T., & Taylor, C. C. (2024). Multivariate analysis. John Wiley & Sons.
[15]. Nuñez Perez, F. A. (2025). Analytical–Computational Integration of Equivalent Circuit Modeling, Hybrid Optimization, and Statistical Validation for Electrochemical Impedance Spectroscopy. Electrochem, 6(4), 35.
[16]. Robinson, S. G., & Sigman, M. S. (2020). Integrating electrochemical and statistical analysis tools for molecular design and mechanistic understanding. Accounts of Chemical Research, 53(2), 289-299.
[17]. Strebl, M. G., Bruns, M. P., & Virtanen, S. (2023). Respirometric in situ methods for real-time monitoring of corrosion rates: Part III. Deconvolution of electrochemical polarization curves. Journal of the Electrochemical Society, 170(6), 061503.
[18]. Sun, J., Sun, S., Yang, X., Xie, F., & Shao, Z. (2025). Investigation on the distribution of dynamic polarization behavior of proton exchange membrane fuel cells based on time resolution electrochemical impedance spectroscopy. Applied Energy, 381, 125111.
[19]. Suzer, S., Strelcov, E., & Kolmakov, A. (2021). Comparative operando XPS and SEM spatiotemporal potential mapping of ionic liquid polarization in a coplanar electrochemical device. Analytical Chemistry, 93(39), 13268-13273.
[20]. Wang, S., Wang, Y., & Soo, Y. Y. (2025). Evaluation and prediction of lithium-ion battery pack inconsistency in electric vehicles based on actual operating data. Energy, 319, 134879.
[21]. Zhu, D., Li, J., Zheng, Z., Ye, S., Pan, Y., Wu, J., ... & Chen, Y. (2024). Water and salt concentration-dependent electrochemical performance of hydrogel electrolytes in zinc-ion batteries. ACS Applied Materials & Interfaces, 16(13), 16175-16185.